JOURNAL OF GEOPHYSICAL RESEARCH, VOL. 104, NO. D22, PAGES 27,321–27,339, NOVEMBER 27, 1999

Effects of solar cycle variability on the lower stratosphere and the troposphere

Nambath K. Balachandran,[1,2] David Rind,[1] Patrick Lonergan,[1,3] and Drew T. Shindell[1,2]

Abstract. The effects of solar irradiance variability on the lower stratosphere and the troposphere are investigated using observed and general circulation model (GCM)-generated 30 and 100 mbar geopotential heights. The GCM includes changes in UV input (+ or −5% at wavelengths below 0.3 micron and no ozone photochemistry and transport) to roughly approximate the combined effects of UV and ozone changes associated with the solar variability. The annual and seasonal averages of the height differences between solar maximum and solar minimum conditions are evaluated. In the subtropics, observations indicate statistically highly significant increased geopotential heights during solar maximum, compared to solar minimum, in composite annual and seasonal averages. The model simulates this feature reasonably well, although the magnitude and statistical significance of the differences are often weaker than in observations, especially in summer. Both the observations and the model results show a strong dipole pattern of height differences when the data are partitioned according to the phase of the quasi-biennial oscillation (QBO), with the pattern reversing itself with the change in the phase of the QBO. The connection between solar variability and lower atmospheric changes are interpreted as follows: The solar changes directly affect the stratosphere by changing the vertical gradients of temperature and zonal wind. This leads to changes in propagation conditions for planetary waves resulting in changes of E-P flux divergence and then by the downward control principle, affecting the circulation in the lower stratosphere and the troposphere.

1. Introduction

The idea of the association between the variation of the radiative output of the Sun during the solar cycle and the tropospheric circulation is a controversial one. The main reason for this controversy is that the percentage change of the total solar radiation is too small to directly affect the massive tropospheric system [*National Research Council* (*NRC*), 1994]. The change in the ultraviolet (UV) range of the radiation, however, is significant, but this radiation directly affects only the stratospheric regions. So, if the solar variation affects the troposphere significantly, it has to be an indirect effect.

A modulation of solar effects by the quasi-biennial oscillation (QBO) of the equatorial stratosphere has been reported by *Labitzke* [1982, 1987, 1992] and *van Loon and Labitzke* [1988] (hereinafter referred to as LvL). They reported that linear correlation studies between the solar cycle changes and the high-latitude stratospheric temperatures and geopotential heights show no association; but when the data are stratified according to the east or west phase of the QBO, significant correlations are found. They reported that when the QBO was in its west phase, the polar data were positively correlated with the solar cycle and when in its east phase, negatively correlated. *Naito and Hirota* [1997] essentially confirmed these findings. Earlier, *Holton and Tan* [1980, 1982] had shown that polar regions were warmer during the east phase of the QBO, with higher geopotential heights, while low latitudes had reduced temperatures and heights, compared to the west phase of the QBO. No effects due to solar variability were reported. *Naito and Hirota* [1997] reported that the *Holton and Tan* [1980] data were essentially confined to solar minimum conditions and when data for solar maximum conditions was also included, then the analysis agreed with LvL findings. With the use of a middle-atmosphere general circulation model (GCM) and +5% and −5% UV change (for wavelengths less than 0.3 microns) to correspond crudely to solar maximum and solar minimum conditions (for the 11-year activity cycle of the Sun) respectively, and forcing the equatorial wind to QBO conditions, *Balachandran and Rind* [1995] have found general agreement with LvL findings of high-latitude lower-stratospheric warming and cooling for combinations of UV change and QBO phase. *Rind and Balachandran* [1995] reported that tropospheric effects of solar variability also occurred in the model.

LvL found, in addition, that lower stratospheric geopotential height also correlates with the solar cycle such that ridges tend to be more pronounced in the subtropics under solar maximum conditions. This correlation does not require separation of the data according to the phase of the QBO. The maximum correlation of geopotential height with solar 10.7 cm flux occurs near 30 mbar and near 30° latitude in both hemispheres. *Labitzke and van Loon* [1997] found a similar correlation of total ozone with solar flux and suggested that ridges formed in the subtropics may present barriers for the poleward transport of ozone. The ridges, rather than being direct barriers to ozone transport, may be a manifestation of the change in meridional circulation and downward motion in the subtropics which con-

[1]NASA Goddard Institute for Space Studies, New York.
[2]Also at Center for Climate Systems Research, Columbia University, New York.
[3]Also at Science Systems and Applications, New York.

Paper number 1999JD900924.
0148-0227/99/1999JD900924$09.00

fines tracers in the tropics. The transport conditions for ozone may have implications for the higher-latitude ozone depletion. *Grant et al*. [1996] and *Trepte and Hitchman* [1992] have discussed the seasonal variation of tropical stratospheric reservoir and the effects of equatorial QBO on normal barriers to transport. The solar variability may also be a factor in the above processes.

In the present study we report lower-stratospheric geopotential height changes associated with solar variations and the QBO for both observations and model simulations. Since the geopotential height changes of a pressure level will include the cumulative effect of temperature changes in the layer below, it may be more responsive to solar variability than just the temperature structure at a particular level.

The model used in this work is the GISS Middle Atmosphere Model (GCMAM) with $8° \times 10°$ (latitude $\times$ longitude) horizontal resolution. The model has a vertical resolution of about 5 km in the stratosphere and extends to a height of about 85 km. Full details of the model are given by *Rind et al*. [1988a, b]. This model does not include ozone chemistry and transport. The ozone distribution is specified using climatological means. Results from using realistic UV and ozone anomalies from an off-line interactive two-dimensional (2-D) model in the GCMAM have been reported by *Shindell et al*. [1999]. However, results obtained by using a flat 5% UV change provide the best agreement with observations. Development of a GCM with fully coupled chemistry and ozone transport has been initiated at GISS.

2. Data

Both observational data and data generated by model simulations of geopotential heights and temperatures are utilized for this work. The observational data are provided by the Free University of Berlin. For the model the solar maximum and minimum conditions are simulated by increasing the solar radiation input (below 0.3 microns) by 5% and decreasing by 5%, respectively. Even though this change appears to be large in the longer-wavelength region of the spectral range, it should be noticed that the UV change brings about ozone changes in the middle atmosphere. *Haigh* [1996] has reported good model simulations of surface temperature changes due to solar variation by incorporating both UV and ozone changes in the model. In our case, the crude 5% UV change seems to simulate the combined temperature effect of solar UV change and the associated ozone change reasonably well. For comparison, see *McCormack and Hood* [1996, Figure 6a] for observations and *Balachandran and Rind* [1995, Figure 9 (top right)]; in general, the magnitudes of the temperature differences are comparable, with the 1°C isotherm located around 30 km height for both the observations and the model.

The model uses climatological means for ozone distribution with no interactive ozone chemistry and transport changes with solar variability. We have done computations with accurate spectral changes and ozone distribution changes from an interactive two-dimensional model [*Shindell et al*., 1999], producing temperature responses of less magnitude than those calculated here. Uncertainties exist in that approach as well; for example, the calculated ozone changes in the lower stratosphere are greater than those from satellite observations, as reported by *McCormack and Hood* [1996], while the upper stratospheric changes are less. Therefore as an alternative, in this paper we utilise the slightly higher UV forcing and leave the ozone unchanged. It may also be pointed out that only limited amounts of data of UV and ozone change over the solar cycle are available.

Note that from a total energy standpoint the UV change applied does not exaggerate the solar forcing. Recent measurements [*Frohlich and Lean*, 1998] show that the total solar irradiance levels increased by 0.1% from solar minimum to solar maximum. Since the UV component (wavelengths less than 0.3 microns) is about 1% of the total solar irradiance [*NRC*, 1994], the 10% (from solar minimum to maximum) UV change we have used in the GCMAM amounts to about 0.1% of the total solar irradiance.

The simulations also include a QBO, which is forced in the model as described by *Balachandran and Rind* [1995]. Results are shown with respect to the QBO phase and averaged over it.

The observational data consist of monthly averages of temperatures and geopotential heights for 27 years (1970–1996). The data were first partitioned between solar maximum and solar minimum conditions without regard for the QBO phase. Then the data for each maximum and minimum was partitioned according to the phase of the QBO. To determine the solar effects, geopotential height differences between the solar maximum and the minimum conditions were plotted for annual and seasonal averages and QBO phases. The model data consist of a total of 60 years, with data for 10 years in each category. Table 1 gives the number of years of observational and model data.

3. Geopotential Height Analyses

Geopotential heights for a particular pressure surface give the cumulative effect of the temperature structure between that surface and the ground level. As such, geopotential height changes may be more apparent than temperature change at a particular level. There is, of course, the possibility that the temperature changes in different layers may be in the opposite direction and may produce a cancellation of the effects. Below we investigate the geopotential height changes associated with solar and QBO variations for different pressure levels.

3.1. The 30 mbar Height Changes

The 30 mbar pressure level corresponds roughly to a height of about 24 km in the lower stratosphere. The 30 mbar geopotential height thus includes the stratospheric region of maximum ozone concentration. *Labitzke and van Loon* [1997] and *van Loon and Labitzke* [1998] have computed the correlation between the 10.7 cm solar flux and 30 mbar geopotential heights. In this paper we will analyze the height differences between the solar maximum and minimum conditions simulated by the model and compare the results with observations.

The observational results are not qualitatively different

Table 1. Number of Years of Data in Each Category

	Observations	Model
Solar maximum	7 (QBO phase ignored)	10 (no QBO)
Solar minimum	13 (QBO phase ignored)	10 (no QBO)
Solar max. E QBO	4	10
Solar max. W QBO	4	10
Solar min. E QBO	6	10
Solar min. W QBO	5	10

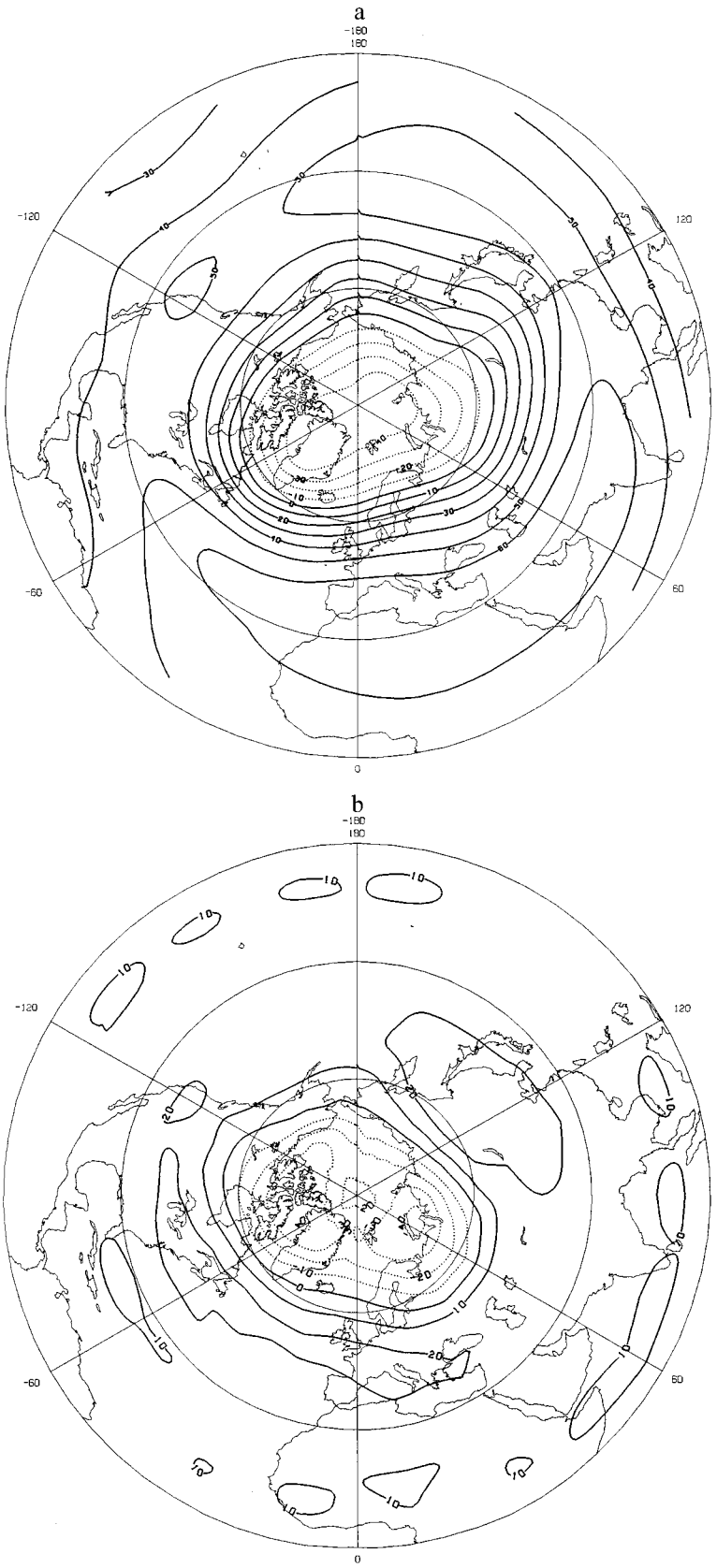

Figure 1. Composite annual averages of 30 mbar geopotential height differences (solar maximum minus solar minimum) for the Northern Hemisphere for (a) observations and (b) model. The contour interval is 10 m.

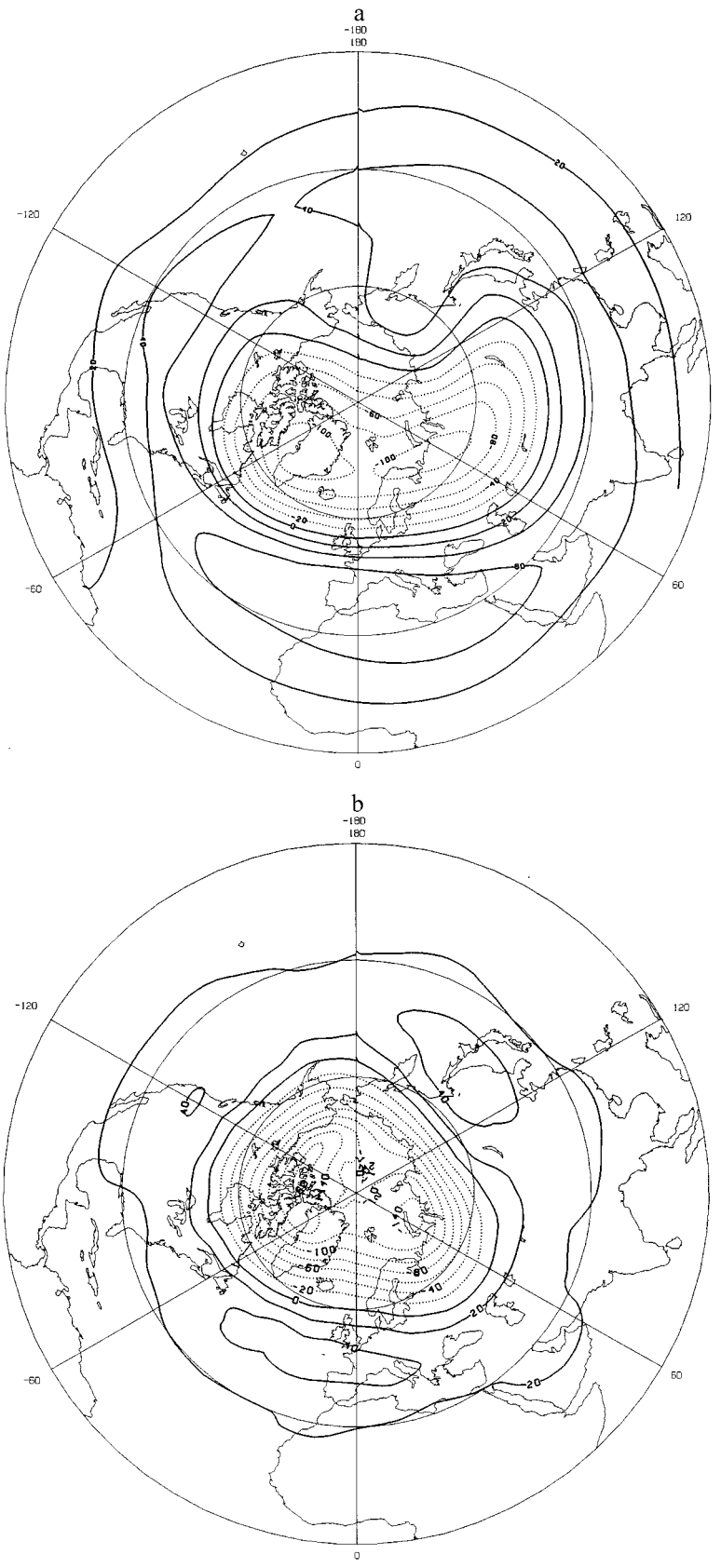

Figure 2. Same as in Figure 1 but for December–January–February averages. The contour interval is 20 m.

when other data sets are used. For example, *van Loon and Labitzke* [1999] report that when using data from the National Centers for Environmental Prediction/National Center for Atmospheric Research (NCEP/NCAR) reanalysis, the solar signal is even stronger than in the Berlin data.

Figure 1a shows the observed average annual 30 mbar height differences (solar maximum minus solar minimum) for the Northern Hemisphere without considering QBO phases. Figure 1b shows the same height differences from model computations. Both the observations and the model simulations show that the geopotential heights are lower near the pole (and hence colder average temperature in the layer) and higher at lower latitudes (warmer average temperature in the layer) for the solar maximum compared to the solar minimum. The minimum value for negative height differences near the pole is < -40 m in both cases. The maximum value of positive height differences (ridges) is >60 m for observations in the subtropics and >20 m for the model in midlatitudes. Thus both the observations and the model are showing a qualitatively similar response to solar forcing with the model showing less sensitivity. The ridges have implications for the transport of ozone from equatorial regions to higher latitudes [*Labitzke and van Loon*, 1997; *Randel et al*., 1993].

When we look at the data for winter months (December–February averages), the above pattern becomes much stronger for both observations and the model. Figure 2a shows the 30 mbar height differences for the winter months of the observational data, and Figure 2b shows the corresponding model results. Again, a strong core of lower heights (lower temperatures) near the pole and higher heights (higher temperatures) in the subtropics for solar maximum compared to solar minimum can be seen in observations. A similar pattern with a tighter core of negative contours centered around the North Pole is seen for the model. The minimum negative value is < -100 m for the observations and < -140 m for the model. The maximum value in the ridges is >60 m for observations and >40 m for the model. Thus the height-difference pattern for winter months in the Northern Hemisphere shows that 30 mbar geopotential heights are lower at the polar regions and higher at the subtropics for both the observations and the model. This is in agreement with LvL findings of negative correlations with solar cycle changes in the polar regions and positive correlations in the subtropics. Thus even without partitioning according to the QBO phases, in winter months, there is a noticeable dipolar effect due to solar changes, with different regions of the globe affected differently. The differences between the model and the observations are noteworthy; as we will see later, the negative differences for the observations are not statistically significant, but for the model they are. This may be due to the inadequate generation of planetary waves in the model [e.g., *Rind et al*., 1988a], producing less variability.

When we look at the annual average 30 mbar geopotential height differences for the easterly (E) QBO case, the observational data show a similar pattern to the unpartitioned data in Figure 1a but much stronger. The minimum height difference near the pole is < -120 m, whereas in Figure 2a, it is only < -40 m. The model results differ, showing a much weaker pattern than the data without any QBO forcing in Figure 1b. This, as we will see later, is because compared to observations, the model does not reproduce the solar effects in seasons other than the winter.

The winter data (DJF) for the E-QBO case is presented in Figure 3. The observational data (Figure 3a) show a strong elongated negative height difference pattern in the polar region with a minimum value of < -180 m; the model data (Figure 3b) show a double minimum near the pole with a value of < -120 m. In both cases, stronger subtropical ridges compared to earlier plots are present. In the subtropics the positive height differences with a maximum value of >80 m are present for both the observations and the model. The troughs and ridges are spread out over almost the whole hemisphere in observational data, whereas they are more compact for the model. In general, when compared with observations, in this E-QBO case, the model generates a reasonable simulation of the geopotential height differences between the solar maximum and the solar minimum conditions.

When we consider the W-QBO case, a reversal of the dipolar pattern of the E QBO is seen in annual averages for both the observations and the model. In both cases the height differences near the pole are positive (indicating higher heights for solar maximum compared to solar minimum) as opposed to negative height differences for the E-QBO case. In the subtropics the observational data indicate a minimum increase, while the model has troughs. If instead of annual averages we consider just the winter data (DJF) in Figure 4, a stronger antisymmetric pattern to that of the E-QBO case is clearly seen. In Figure 4a the observational data show strong positive height differences centered roughly about the pole and extending to the middle latitudes. The maximum height difference, located near the pole, is >500 m, and negative height differences (troughs) located in the middle latitudes are also present. This pattern is simulated well in the model (Figure 4b), but the maximum value of the differences near the pole is only >210 m. The minimum values in the subtropical troughs are < -80 m for observations and < -50 m for the model. Thus in this case also, the model simulation, while showing the same pattern as observations, is weaker in intensity.

3.2. 100 mbar Height Changes

As we go down to the 100 mbar level (at a height of about 16 km), the general pattern of geopotential height difference distributions remain the same, with the subtropical patterns intensifying and polar patterns weakening, compared to the 30 mbar plots shown above. This indicates the robustness of the solar influence on the lower stratosphere and the troposphere and its potential impact on tracer transport. This also indicates that the main subtropical component of the solar influence may be in the troposphere.

Since the 100 mbar height patterns generally follow those of 30 mbar, we will present the results only for winter months (DJF) when the height differences are the strongest (especially for the model) and also show some variations from the 30 mbar height patterns. Figures 5a and 5b show the winter (DJF) averages for the 100 mbar geopotential height differences for the observational and model data, respectively, without considering the QBO phase. For both the observations and the model the polar lows have weakened and the subtropical ridges have generally remained the same as for the 30 mbar level. The patterns look like the DJF E-QBO pattern seen earlier for the 30 mbar level. The 100 mbar height differences between the solar maximum and the solar minimum for winter months and E QBO are given in Figures 6a (observations) and 6b (model). In both cases the polar lows are reduced in intensity (compared to 30 mbar values), but for the observations, the ridges stretching from high latitudes to subtropics have intensified and troughs have started forming in the tropics. For the W-QBO

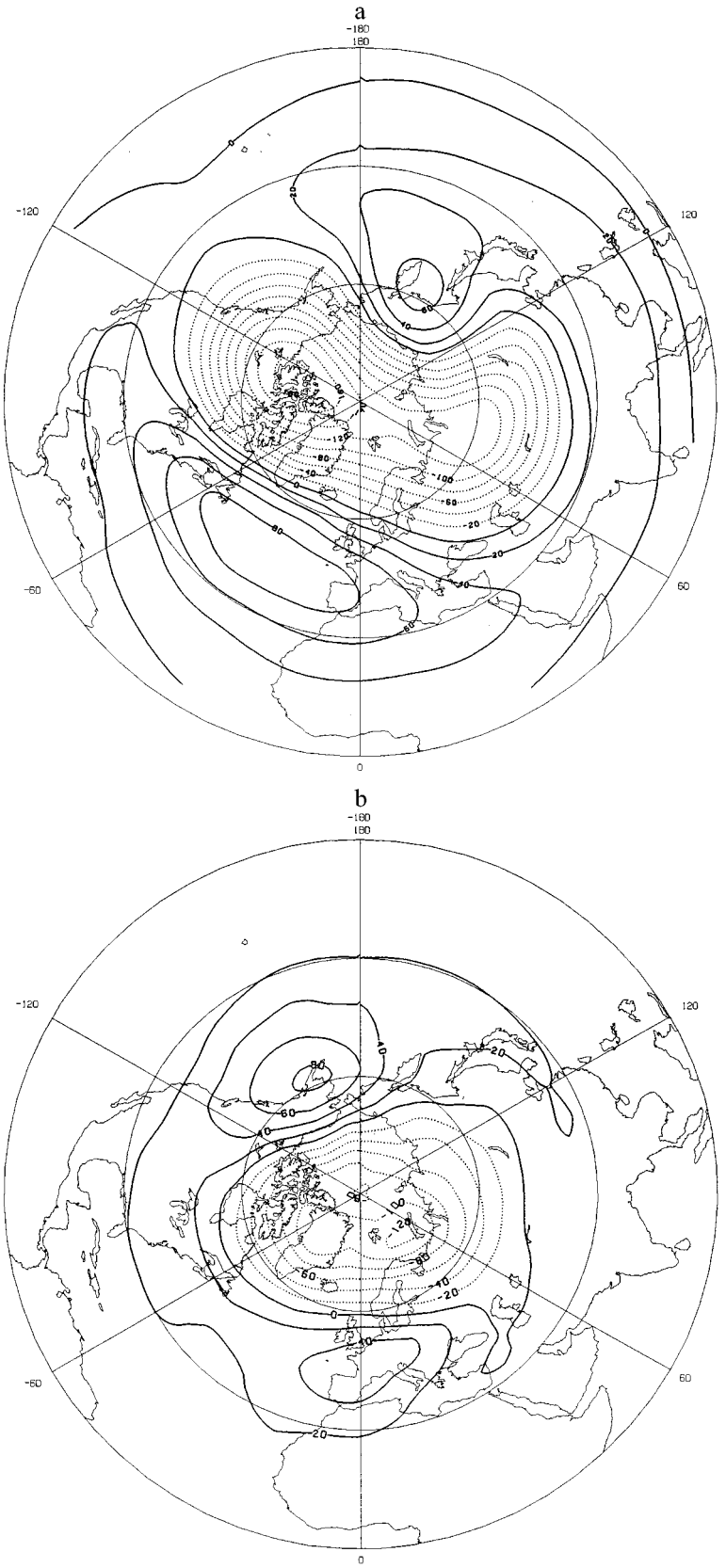

Figure 3. Composite December–January–February averages of height differences for easterly (E) quasi-biennial oscillation (QBO) for (a) observations and (b) model. The contour interval is 20 m.

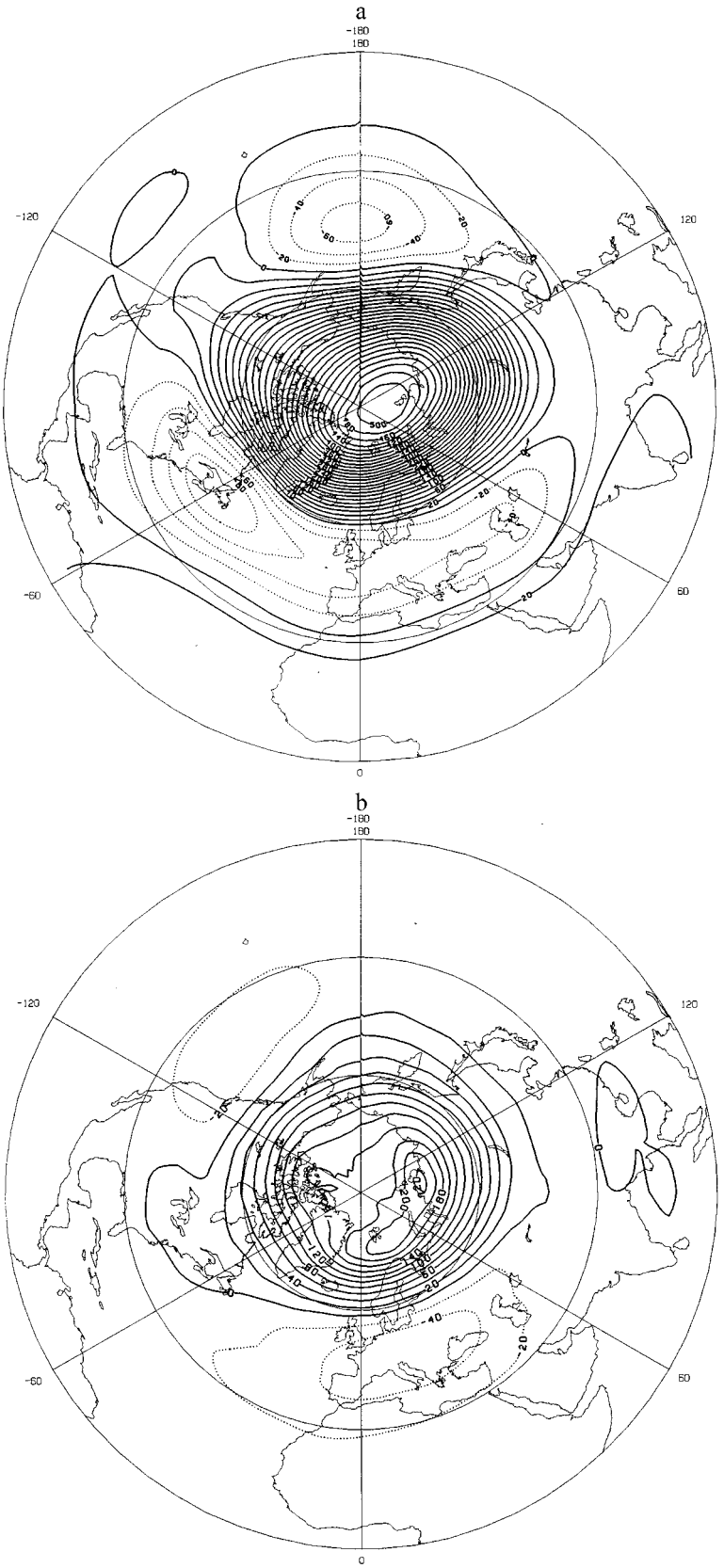

Figure 4. Same as in Figure 3 but for the W-QBO case.

case for winter (Figures 7a and 7b), the polar highs are reduced significantly (compared to the 30 mbar plots in Figures 4a and 4b), and the troughs remain the same. In the observations, ridges are seen in the tropics.

The above analysis appears to indicate a connection between solar radiation changes and geopotential height changes in the lower stratosphere and troposphere. The geopotential height difference between solar maximum and solar minimum shows a dipole pattern with positive (negative) height differences centered at the pole and negative (positive) height differences in the subtropics for westerly (easterly) QBO. This agrees with the Labitzke and van Loon findings of positive correlation of 10.7 cm solar flux with polar temperature in the stratosphere during the W QBO and negative correlation during the E QBO. Exactly a reversed height difference pattern to that in the polar regions exists in the subtropics. When we take the composite yearly average without considering the phase of the QBO, the pattern is generally that for the E QBO.

4. Statistical Significance of the Height Differences

From the data presented above, the geopotential height differences in the lower stratosphere associated with the solar variability appear to be robust. However, how statistically significant are these height differences between the solar maximum and the minimum conditions? The northern polar data during winter is especially noted for great variability, and the results are to be treated with caution before we reach any conclusions about the solar connection. Further, in regions like the tropics where we do not see high values for the height differences, the small differences which are unnoticeable may be statistically significant, because the variability also is small. To evaluate these results, each of the data sets for solar maximum and minimum conditions were tested for the significance of the difference of their means by applying "student's" t test [*Brooks and Carruthers*, 1953].

4.1. Annual Patterns

Figures 8a and 8b show the t values for the observations and model data, respectively, of annual mean 30 mbar height differences. The most striking feature of the observations (Figure 8a) is the high values of t centered roughly just below the 30°N latitude circle. The model data (Figure 8b) also show high values of t centered about the 30°N latitude circle, although the values are not so large as in the observations. The negative t values centered about the pole are somewhat larger in magnitude for the model than for the observations.

To test the statistical significance of the difference in geopotential heights between the solar maximum and minimum conditions, we use the Fisher and Yates statistical tables [*Brooks and Carruthers*, 1953, p. 383]. Each observational and model data set of annual means (without partitioning according to the QBO phases) has 18° of freedom, and a t value of 3.92 is significant at the 99.9% level (in other words, for this t value, the probability that we get the corresponding geopotential height difference by chance is 1 in 1000!). The maximum t values for observations in Figure 8a near the 30°N latitude circle is >6.5 in two regions and >8.5 near 80°E longitude. Thus these height differences are highly significant statistically. The maximum numerical value of t for negative height differences near the North Pole is ~ 1. This turns out to be less significant than even at the 90% level. To be significant at the generally acceptable 95% level, the t values must be at least 2.1. Thus from Figure 8a we see that significantly increased annual averages of 30 mbar geopotential heights are observed during the solar maximum compared to the solar minimum from middle to tropical latitudes in the Northern Hemisphere. The significance reaches maximum in the subtropics roughly coinciding with the maximum in actual geopotential height differences (Figure 1a).

When we look at the t plots for the model data (Figure 8b), we see the same highly significant height differences in the subtropics with more-or-less the same latitudinal and longitudinal distribution of the peak values of t. Even though the maximum values of t for the model are less than those for observations, the model values are still significant at the 99.9% level in some regions. The main difference for the model data is that significant negative values are seen near the pole. These reduced heights for the solar maximum compared to the solar minimum are significant at the 95% level in some regions near the pole.

4.2. Seasonal Patterns

Next, we consider the t plots for the seasonal averages of the height differences. During the winter (DJF) months for the observations and the model, the patterns are, in general, similar to the patterns for the annual average plots (Figure 8), except that for the observational data, the t values are reduced by more than 50% but still highly significant statistically. For the spring (MAM) months also we notice the persistence of the patterns of the annual and winter averages with significant ridges in the subtropics. The statistically significant negative height differences near the pole are not present in the spring for the model. Figure 9 shows the t plots for the summer (JJA) months for observations. The most striking result is that for the observational data, statistically significant higher geopotential heights for the solar maximum are present from the high-latitude regions to the tropics. The t values again peak at the subtropics, and these peaks for summer are higher than those for the winter and spring. The model does not properly reproduce these statistically significant height differences for summer. The t plots for the fall (SON) months, again, show for observational data significant positive values from midlatitudes to the tropics with highly significant ridges in the tropics and subtropics. There is an indication that ridges have moved slightly toward the lower latitudes. The model plots generally agree with these patterns with the ridges located in the subtropics.

The pattern emerging from the above analysis is one of generally increased 30 mbar geopotential heights for the solar maximum conditions compared to solar minimum conditions with ridges in the subtropics; the polar pattern is often not significant. The patterns generated by the model are weaker than in the observations, but the model shows a similar dipole pattern with negative values near the pole and positive values at lower latitudes. The model does not reproduce the height differences for the summer properly.

4.3. QBO Effects

Figures 10a and 10b show the t plots for the height differences (annual averages) between the solar maximum and minimum conditions for the E-QBO case for observations and model runs, respectively. Ridges north of 30°N latitude are clearly discernible in both diagrams. The number of degrees of freedom for the observational data (Figure 10a) is 8, and here, t values over 2.31 are significant at the 95% level, while values

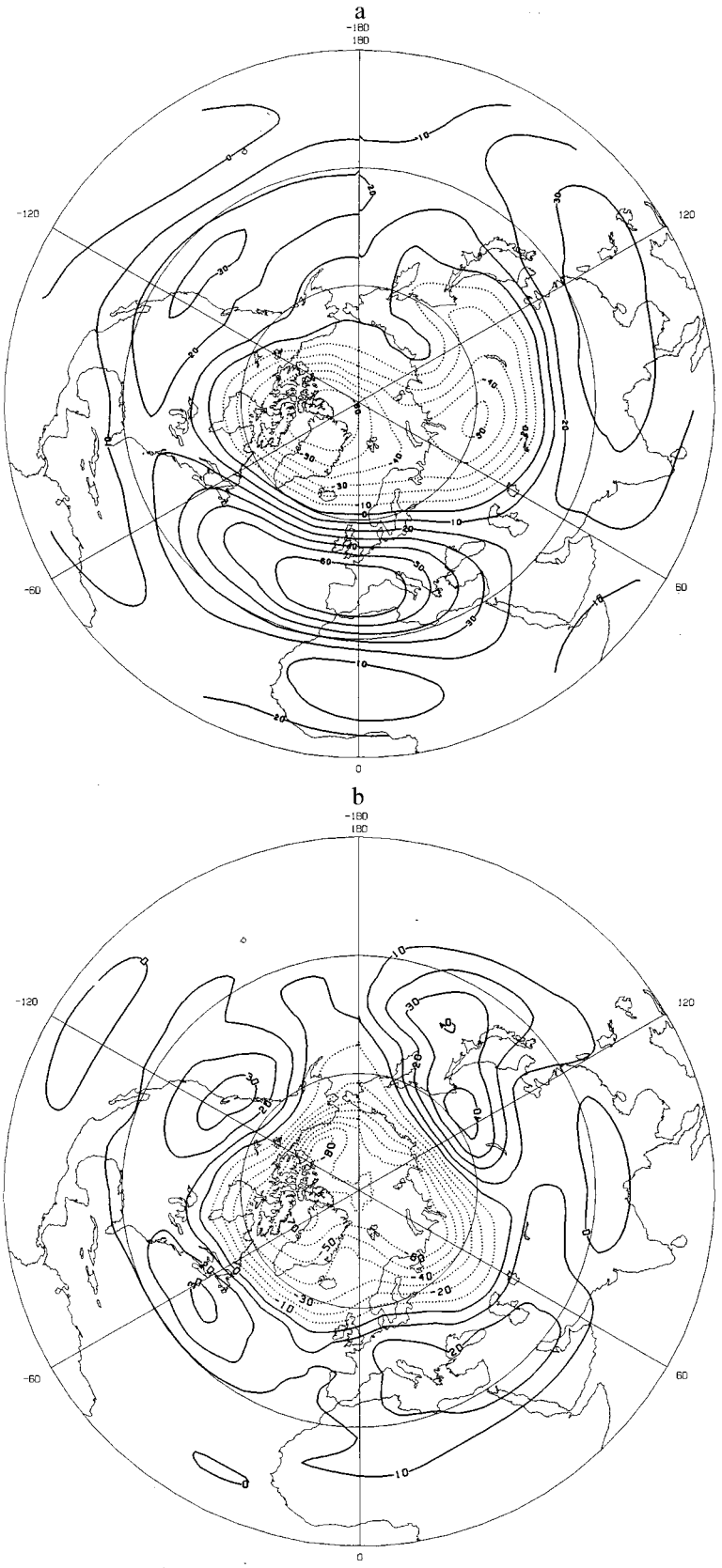

Figure 5. Same as in Figure 2 but for 100 mbar geopotential heights. Contour interval is 10 m.

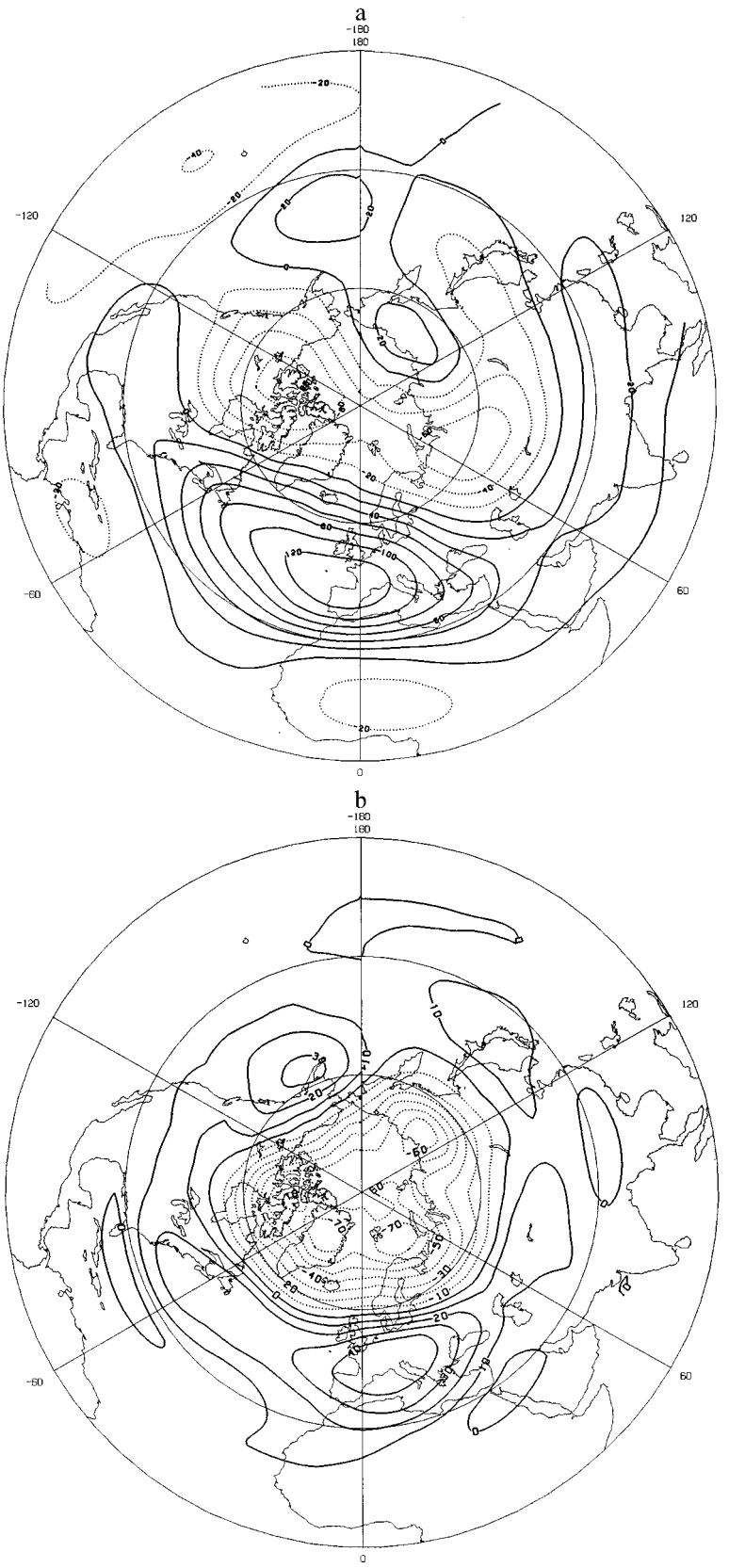

Figure 6. Same as in Figure 5 but for the E-QBO case. Contour intervals: (a) 20 m and (b) 10 m.

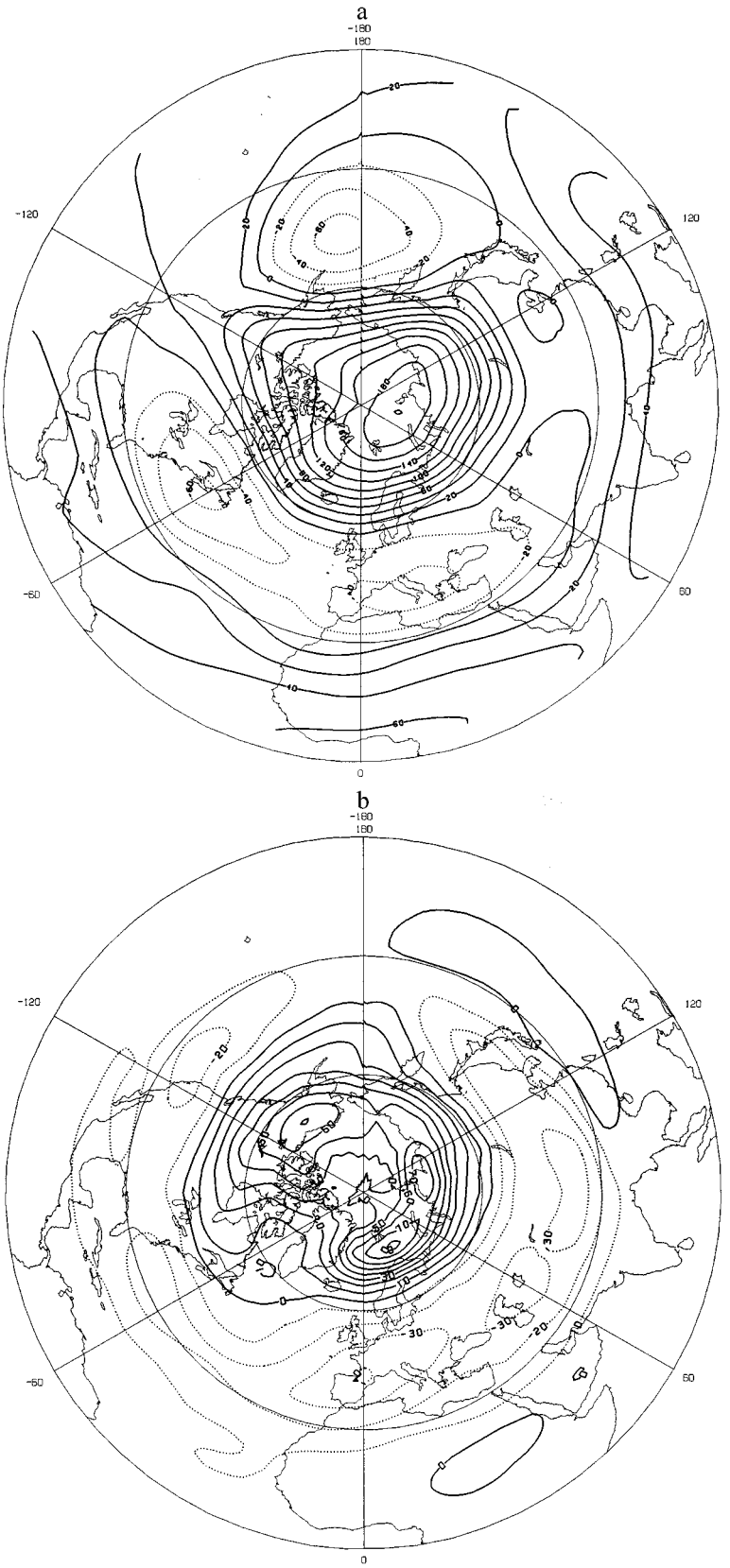

Figure 7. Same as in Figure 6 but for W-QBO.

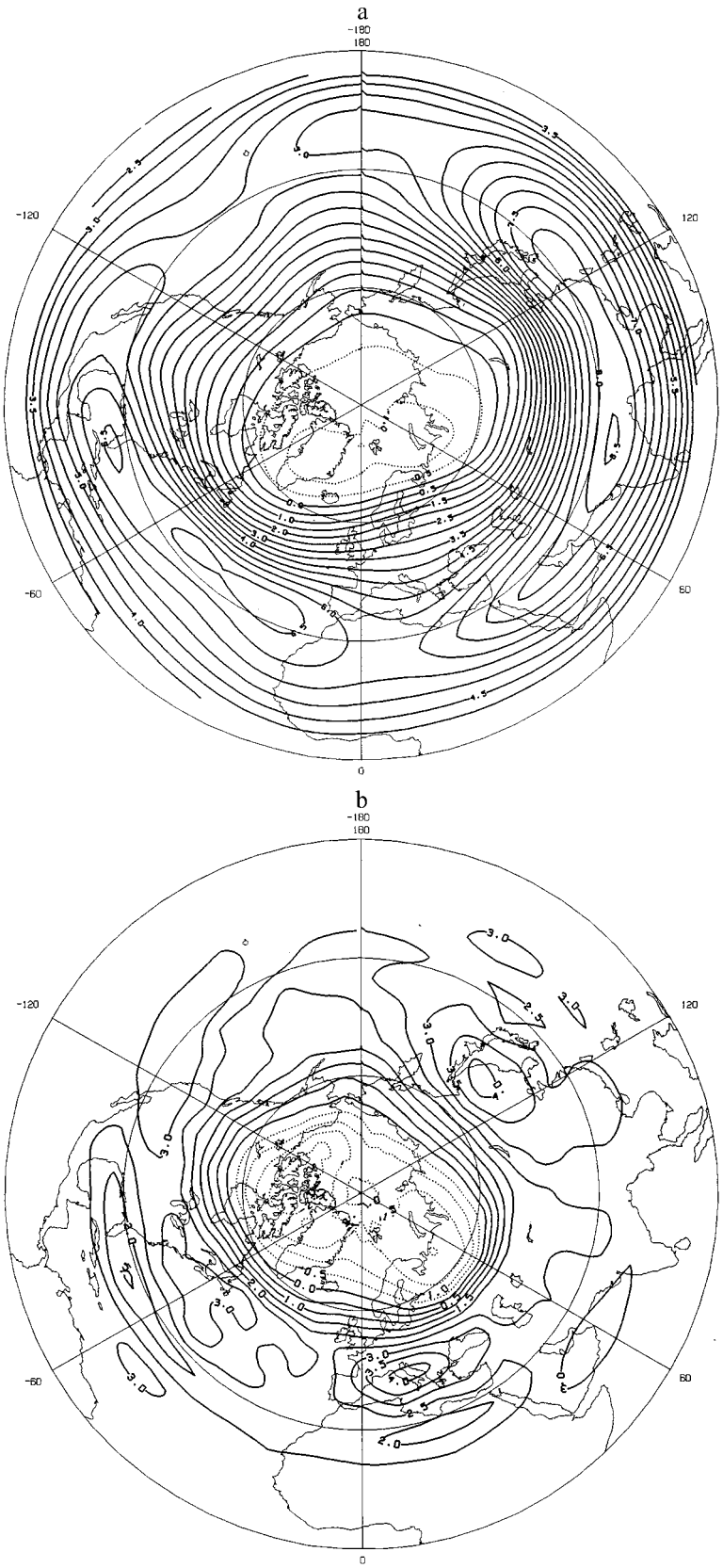

Figure 8. Values of "student" t for annual averages of 30 mbar height differences between solar maximum and solar minimum (a) for observations and (b) for the model. Contour interval is 0.5.

over 3.35 are significant at the 99% level. The peak value of t is >4.0 near the Greenwich meridian with values of >2.5 and >3.5 at other locations. The negative values near the pole are not significant for the observations. For the model data with 18° of freedom the negative values near the pole are still not significant at the 95% level. Values >2.10 are significant at the 95% level, and >2.88 are significant at the 99% level. For the model the peak t value is >3.0 near the Greenwich meridian with values of >3.0 and >2.5 at other locations. Thus the positive height differences north of 30°N are statistically significant for both the observational and the model data.

Figures 11a and 11b show t values for the annual average height differences for the W-QBO conditions for the observations and model, respectively. What we notice when we compare data for different QBO phases in Figures 10 and 11 is that in the W-QBO case, the ridges have moved toward the equator compared to the E-QBO case, for both observational and model data. The model shows some statistically significant troughs in the middle latitudes for the W QBO, which are absent in the observational data. Also, as in the previous cases, the observational data show stronger ridge patterns than the model data.

For observational data with 7° of freedom, for 95% level of significance, $t = 2.37$, and for 99.9% level, $t = 5.41$. It may be noticed from Figure 11a that the t value for the 99.9% level is exceeded in the tropics. For the model, the height differences in the tropics are significant at the 98% level.

What seems to be clear from the above analysis is that there is evidence for ridge formation in the tropical-subtropical region during the solar maximum compared to the solar minimum irrespective of the seasons and QBO phases. Roughly centered around 30°N latitude, these ridges move toward higher and lower latitudes under different background conditions. For example, when we compare the conditions for different QBO phases, the ridges move toward the equator during the QBO west phase compared to the QBO east phase. This is an indication that the ridges are formed in the regions of planetary wave breaking or surf zone [*McIntyre and Palmer*, 1983]. Since the surf zone is related to the zero wind line, it is reasonable to expect the surf zone to be further equator-ward during the QBO west phase compared to the QBO east phase. In the model, even though reproduction of these observations is reasonably good, the patterns are weaker. This may be due to the fact that planetary wave generation in the model is weaker due to low resolution.

5. Solar Variability and Lower Atmospheric Changes, the Connection

Now we come to the crucial question: What is the explanation for the 30 and 100 mbar height increases in the subtropics for solar maximum conditions compared to solar minimum conditions?

Van Loon and Labitzke [1994] have successfully used station data to illuminate the difference between solar maximum and minimum in the tropospheric column in the tropics and subtropics. They report that the interannual variation of the tropical and subtropical vertical motions (the Hadly circulation) contains a component on the 10–12 year scale; but the mechanism that connects the solar and atmospheric oscillations needs to be discovered.

To investigate the mechanism by which solar irradiance differences between the solar maximum and the minimum affect the lower stratosphere and troposphere, we have to use the model data since the observational data do not provide enough information for such an analysis. Since there is general agreement between the observations and our model results in the pattern of geopotential height differences between the solar maximum and the minimum conditions, the investigations using the model should give us an insight into how the solar UV changes can affect the lower atmosphere.

To study the change in meridional circulation patterns associated with the solar variability, we use the transformed Eulerian mean formulation given by *Andrews and McIntyre* [1976] and commonly used for tracer transport studies [e.g., *Brasseur and Madronich*, 1992]. According to these authors the transformed circulation in the meridional plane accounts for all the mass and energy transport and, under most circumstances, is very similar to the Lagrangian transport of air parcels. We use the TEM formulation because this circulation is driven by the wave drag.

Figure 12a shows the plot of the differences (annual averages) of a transformed Eulerian stream function between the solar maximum and minimum conditions for the model. The figure indicates stronger clockwise circulation for the solar maximum between ~15°N and 50°N with more downward motion (vertical streamline) between ~20°N and 30°N between about 200 and 700 mbar pressure levels. This downward motion can bring about increased temperatures and geopotential heights leading to the ridges seen in Figures 1a and 1b. The transformed stream function data for the Northern Hemisphere winter months are shown in Figure 12b, and we notice that the circulation differences have roughly the same pattern as for the annual averages but have intensified. When we compare the height difference patterns in Figures 1b and 2b, there also we see the same patterns for the ridges for both annual and winter averages with intensification during the winter months.

To further investigate how differences in transformed Eulerian stream function reflect the differences in height changes for the different QBO phases, we will look only at the data for winter months since the model data show strong patterns mainly for the winter months. Figures 12c and 12d present the transformed stream function differences for E QBO and W QBO, respectively. Comparing these two figures, we notice a reversal of the circulation pattern from one QBO phase to the other. Going back to Figures 3b and 4b for the corresponding height plots, there also we see a reversal of the geopotential height difference patterns between the two plots. More specifically, roughly between 25°N and 35°N, we notice a downward motion in the E-QBO case (Figure 12c) and an upward motion for the W-QBO case (Figure 12d). In the geopotential height plots we see ridges in this region for the E QBO (Figure 3b) and troughs for the W QBO (Figure 4b). Thus it appears that ridges in height difference plots are seen in regions where the transformed stream function indicates a relative downward motion and troughs in regions where the stream function indicates an upward motion.

The logical interpretation of the above analysis indicates that the geopotential height changes associated with solar UV changes are related to direct zonal mean meridional circulation changes as indicated by the changes in the transformed stream function. In solar maximum conditions there appears to be more downward motion in the subtropics leading to increased geopotential heights in the lower stratosphere and the

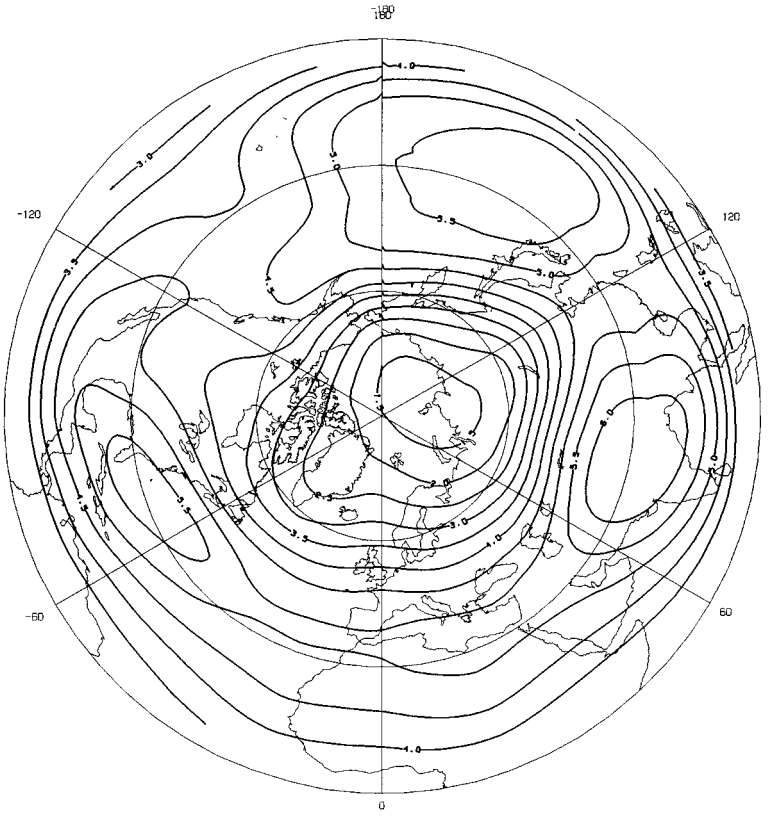

Figure 9. Same as for Figure 8a but for the seasonal average of June–July–August.

troposphere, compared to solar minimum conditions. So the connection between solar irradiance changes and changes in the lower atmosphere seems to be via zonal mean circulation changes.

The question arises as to how the mean circulation in the lower atmosphere is altered by changes in solar irradiance in the UV range. *Balachandran and Rind* [1995] pointed out that solar UV changes which directly affect the middle and upper stratosphere affect the propagation and dissipation of planetary scale waves in the stratosphere. In that paper it was shown that the QBO affects the horizontal gradient of the zonal wind as well as the position of the zero-wind line, whereas the UV change affects the vertical gradients of the zonal wind in the stratosphere. These effects control the propagation and dissipation of planetary waves and thus the Eliassen-Palm (E-P) flux divergences. It was shown that such wind gradient changes and associated refractive index changes can explain the high-latitude lower-stratospheric warmings and coolings associated with solar variability and QBO phase changes as reported by LvL and shown by our model results.

Haynes et al. [1991] have enunciated the "downward control principle" according to which the wave dissipation in a region of the atmosphere will be accompanied by circulation changes in the region below, up to a few scale heights. *Holton* [1990] and *Rosenlof and Holton* [1993] used this principle to calculate the residual mean circulation for the lower stratosphere and troposphere using observational data. *Scol and Yamazaki* [1998] used the above approach to calculate the residual mean circulation and to estimate the mass flux changes at 100 mbar associated with the phase changes of the QBO.

Thus we propose that the way solar irradiance changes affect the lower stratosphere and the troposphere is through changes in the dissipation of planetary scale waves in the middle atmosphere which in turn affect the mean meridional circulation at lower levels (as shown in Figure 12) in accordance with the downward control principle.

The solar variability also appears to affect the Hadley cell in the troposphere. Figure 13 (top) shows the annual average stream function change (solar maximum minus solar minimum) for the model, and Figure 13 (bottom) shows the corresponding precipitation change (times 10). The increased Hadley circulation for the solar maximum is evident in Figure 13 (top) and the tropical precipitation change is evident in Figure 13 (bottom). The precipitation gradients help induce the stream function changes shown in Figure 13 (top). Compared to the mean precipitation values, the changes are small: of the order of a few percent. It would probably be difficult to see such changes in the real world, given the heterogeneous nature of precipitation and the status of precipitation observations. The change is a sizeable fraction of the normal interannual variability of the model, and from this viewpoint, could be important. Being less than a standard deviation, it is not statistically significant; however, in helping to produce the Hadley cell changes, it leads to changes in the subtropical ridges which, at higher elevation, are significant, as shown above. One possible explanation for the Hadley cell change is that the tropospheric circulation change induced by the wave-mean flow interaction in the stratosphere induces precipitation changes, and the associated latent heat release enhances the Hadley cell. Thus it appears that different processes interact to result in the observed effects.

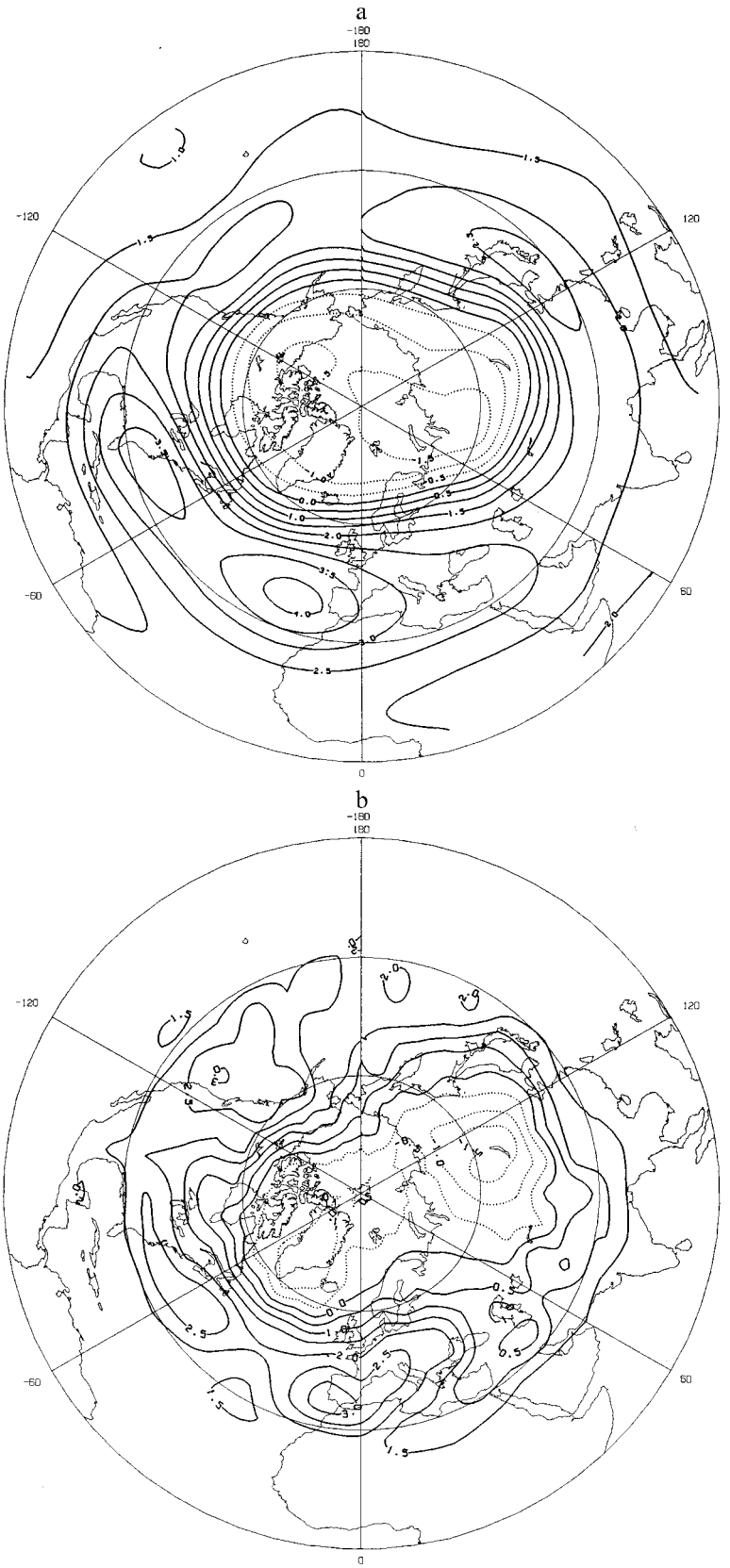

Figure 10. Same as for Figure 8 but for the E-QBO case.

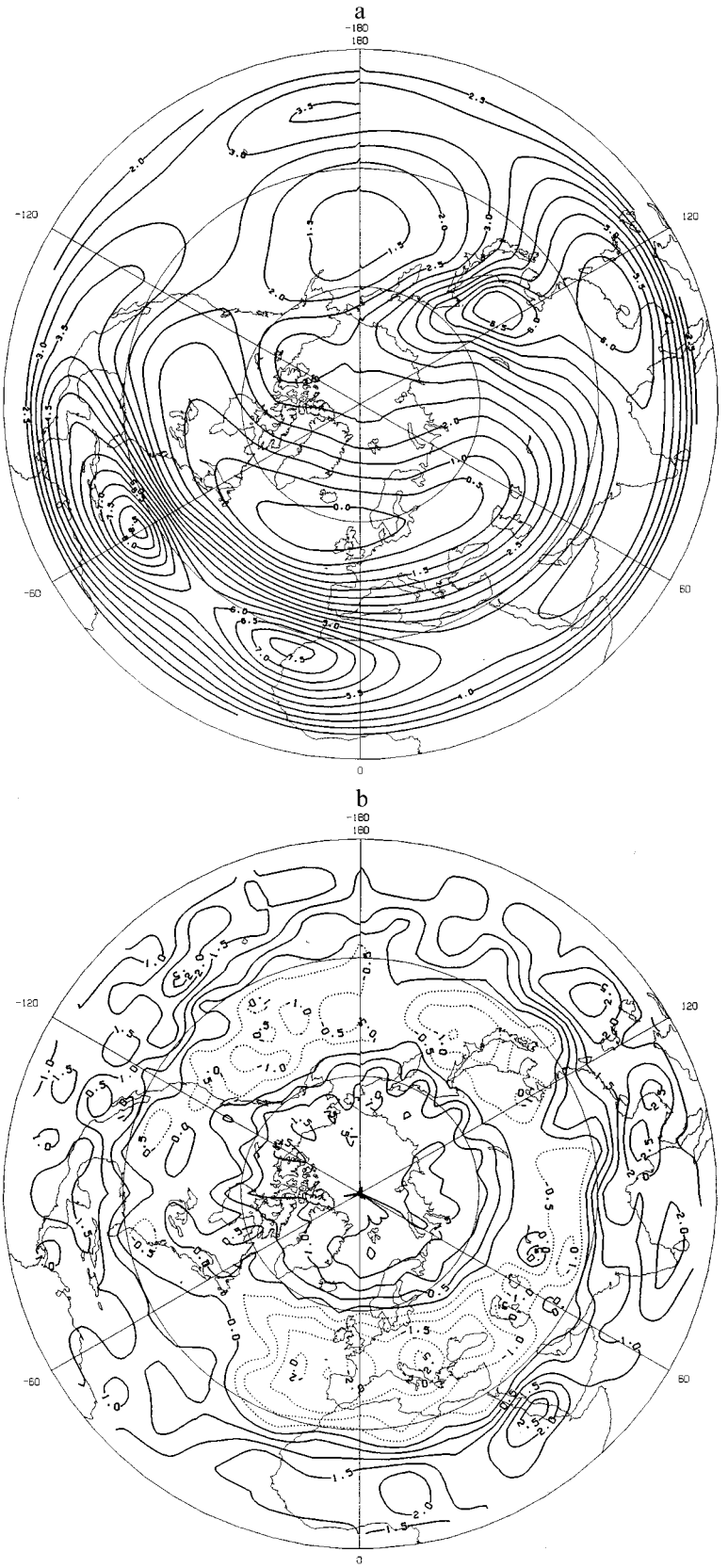

Figure 11. Same as for Figure 10 but for W QBO.

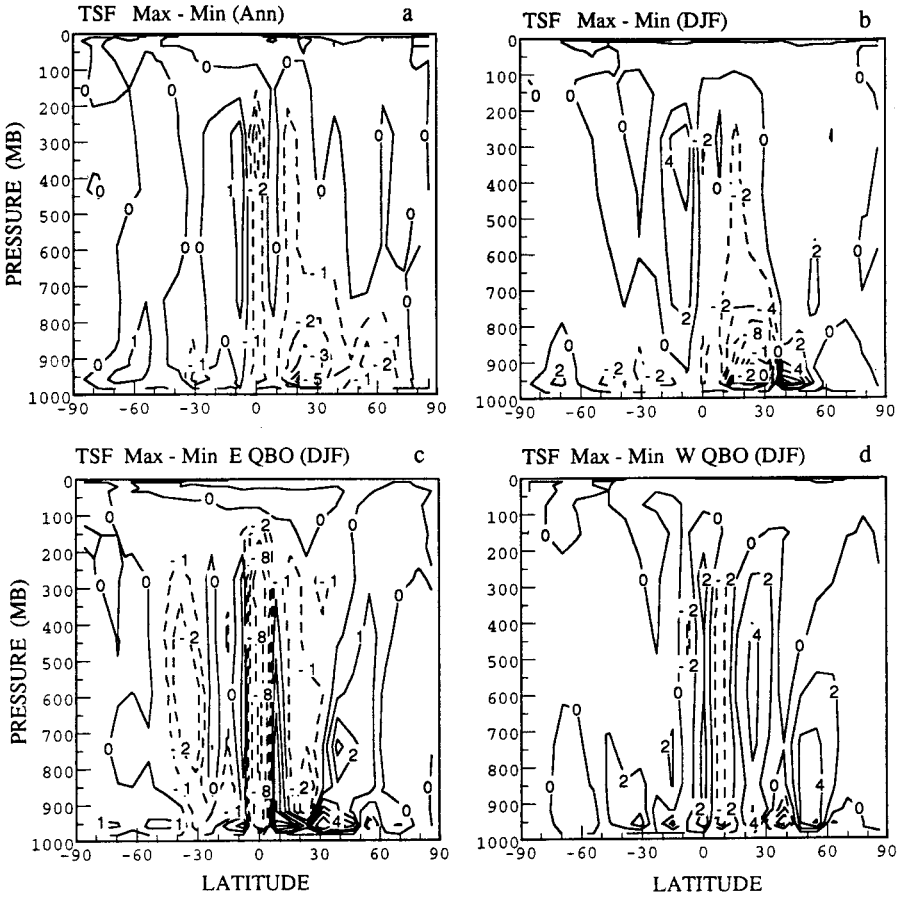

Figure 12. Latitude-altitude plots of the difference in mass stream function of the transformed Eulerian mean meridional circulation between solar maximum and minimum for the model. (a) Annual averages, (b) DJF averages, (c) DJF averages for the E QBO, and (d) DJF averages for the W QBO. The solid lines represent anticlockwise circulation, and dashed lines represent anticlockwise circulation.

6. Summary and Conclusions

We have attempted to explore the connection between solar variability and changes in the lower atmosphere. The pioneering work of Labitzke and van Loon in evaluating correlation between the intensity of 10.7 cm solar radiation and lower atmospheric temperatures has been questioned as to its reliability on signal analysis considerations [e.g., *Salby and Shea*, 1991], including insufficiency of an adequate number of cycles in the data for the solar 11 year periodicity. Recently, however, *Salby and Callahan* [1999] have reported agreement with LvL findings after separating the winter data according to the phase of the QBO. They also report that QBO itself is modulated by the solar cycle! Our attempt in the present work was to compare observational data with model results using the simplest and strongest part of the solar signal, simulate it in the model, and see how the results compare. Thus we chose the solar maximum and minimum conditions (instead of cyclical changes) and investigated how the 30 and 100 mbar geopotential heights, which will show the cumulative effects of solar variability in the lower atmosphere, vary between the two extremes. We also investigated how the equatorial QBO will modulate the solar effects.

Previous attempts by us [*Balachandran and Rind*, 1995] to evaluate the solar connection first concentrated on the Northern Hemisphere polar region, because of the high values of the changes in temperatures in this region. The tropics and subtropics were not considered because the changes there were low. However, the fact of the matter is that the natural variability in the polar regions is also very high and in the tropical and subtropical regions very low. When we consider the statistical significance of the changes, the subtropical effect is emphasized.

We found that both for the observations and for the model, the geopotential height differences between the solar maximum and minimum are statistically highly significant in certain regions. The heights are significantly higher for the solar maximum compared to the solar minimum mainly in the subtropics and tropics. With minor variations this pattern exists for annual averages as well as for all seasonal averages in the observational data. In fact, the composite annual averages show a stronger pattern of such solar connection than for the seasonal averages. This happens not only because the pattern is persistent during all seasons but also because the natural variability is reduced in annual averages. The model results generally agree with observations although the patterns are weaker in the model. The model also does not reproduce the observations for summer. This may be due to the fact that in the model the sea surface temperatures are fixed and not allowed to change with the solar change, limiting the tropospheric response.

The QBO modulates the solar effects on the lower atmosphere. The peak values of the differences in geopotential

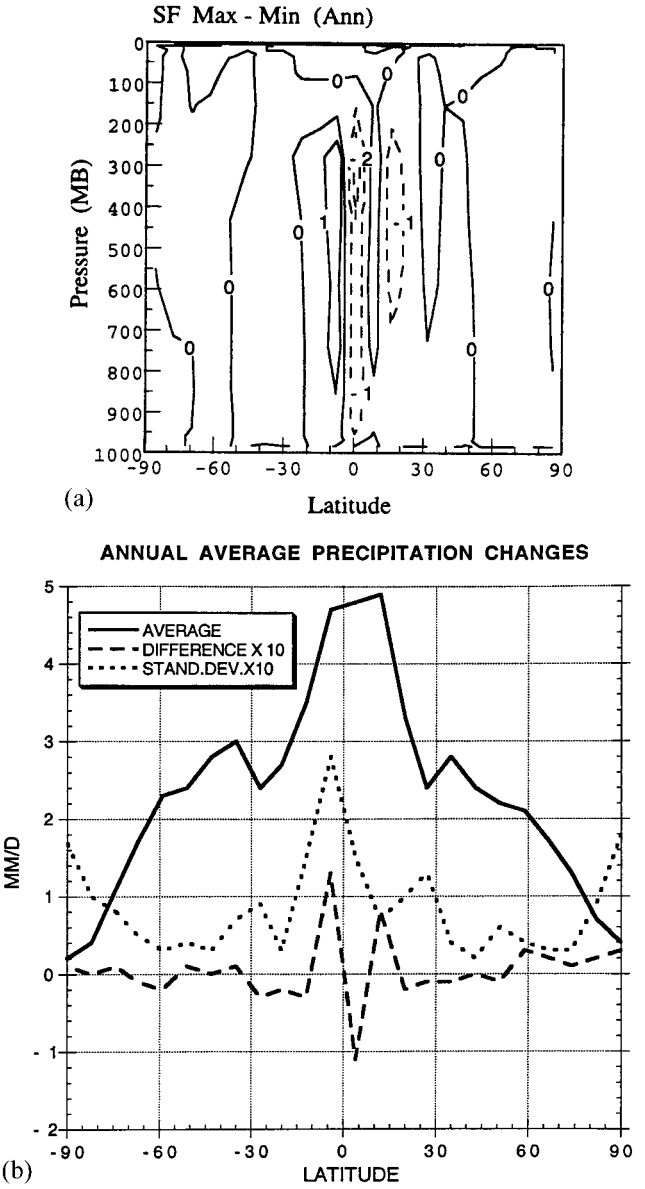

Figure 13. Annual average differences (solar maximum minus solar minimum) for the model for (top) stream function and (bottom) precipitation (×10). Annual average precipitation and standard deviation (×10) are also shown in Figure 13 (bottom).

heights between solar maximum and minimum move to lower latitudes for W QBO compared to E QBO. The height difference pattern also shows a dipole structure between the high and the low latitudes during northern winter with the pattern reversing with the phase of the QBO.

Finally, we conclude that the effects of solar changes on the lower atmosphere may be through changes in direct circulation, as shown by changes in the transformed stream function. According to the "downward control" principle [*Haynes et al*., 1991], when planetary scale waves dissipate in the stratosphere, circulation changes are brought about at the lower levels. We have shown earlier [*Balachandran and Rind*, 1995] that UV changes associated with solar variability bring about changes in the conditions of propagation and dissipation of planetary waves. E-P flux changes associated with the UV changes appear to generate circulation changes in the lower atmosphere along with the temperature and geopotential height differences between the solar maximum and the solar minimum conditions.

Acknowledgments. We are grateful to Harry van Loon at NCAR for helpful comments and discussions. Two anonymous reviewers provided helpful comments. This work was supported by NSF grant ATM9523326, while model development work has been funded by NASA ACMAP.

References

Andrews, D. G., and M. E. McIntyre, Planetary waves in horizontal and vertical shear: The generalized Eliassen-Palm relation and the mean zonal acceleration, *J. Atmos. Sci*., *33*, 2031–2048, 1997.

Balachandran, N. K., and D. Rind, Modeling the effects of UV variability and the QBO on troposphere-stratosphere system, Part I, The middle atmosphere, *J. Clim*., *8*, 2058–2079, 1995.

Balachandran, N. K., R. A. Plumb, R. Suozzo, and D. Rind, The QBO and Stratospheric Warming—Model Results, *J. Geomagn. Geoelectr*., *43*, Suppl., 741–757, 1991.

Brasseur, G. P., and S. Madronich, Chemistry-transport models, in *Climate System Modeling*, edited by K. E. Trenberth, 788 pp., Cambridge Univ. Press, 1992.

Brooks, C. E. P., and N. Carruthers, *Handbook of Statistical Methods in Meteorology*, 412 pp., Her Majesty's Stn. Off., Norwich, England, 1953.

Frohlich, C., and J. Lean, The Sun's total irradiance: Cycles, trends and related climate change uncertainties since 1976, *Geophys. Res. Lett*., *25*, 4377–4380, 1988.

Grant, W. B., E. V. Browell, C. S. Long, L. L. Stowe, R. G. Grainger, and A. Lambert, Use of volcanic aerosols to study the tropical stratospheric reservoir, *J. Geophys. Res*., *101*, 3973–3988, 1996.

Haigh, J. D., The impact of solar variability on climate, *Science*, *272*, 981–984, 1996.

Haynes, P. H., C. J. Marks, M. E. McIntyre, T. G. Shepherd, and K. P. Shine, On the "downward control" of extratropical diabatic circulation by eddy-induced mean zonal forces, *J. Atmos. Sci*., *48*, 651–678, 1991.

Holton, J. R., On the global exchange of mass between the stratosphere and troposphere, *J. Atmos. Sci*., *47*, 392–395, 1990.

Holton, J. R., and H.-C. Tan, The influence of the equatorial quasi-biennial oscillation on the global circulation at 50 mbar, *J. Atmos. Sci*., *37*, 2200–2208, 1980.

Holton, J. R., and H.-C. Tan, The quasi-biennial oscillation in the northern hemisphere lower stratosphere, *J. Meteorol. Soc. Jpn*., *60*, 140–147, 1982.

Labitzke, K., On the interannual variability of the middle stratosphere during northern winters, *J. Meteorol. Soc. Jpn*., *60*, 124–139, 1982.

Labitzke, K., Sunspots, the QBO and stratospheric temperature in the north polar region, *Geophys. Res. Lett*., *14*, 135–137, 1987.

Labitzke, K., and H. van Loon, On the association between the QBO and the extratropical stratosphere, *J. Atmos. Sol. Terr. Phys*., *54*, 1453–1463, 1992.

Labitzke, K., and H. van Loon, Total ozone and the 11-yr sunspot cycle, *J. Atmos. Sol. Terr. Phys*., *59*, 1–9, 1997.

McCormick, J. P., and L. L. Hood, Apparent solar cycle variations of upper stratospheric ozone and temperature: Latitude and seasonal dependens, *J. Geophys. Res*., *101*, 20,933–20,944, 1996.

McIntyre, M. E., and T. N. Palmer, Breaking planetary waves in the stratosphere, *Nature*, *305*, 593–600, 1983.

Naito, Y., and I. Hirota, Interannual variability of the northern winter stratospheric circulation related to the QBO and the solar cycle, *J. Meteorol. Soc. Jpn*., *75*, 925–936, 1997.

National Research Council (NRC), *Solar Influences on Global Change*, 163 pp., Natl. Acad. Press, Washington, D. C., 1994.

Randel, W. J., J. C. Gille, A. E. Roche, J. B. Kumer, J. L. Mergenthaler, J. W. Waters, E. F. Fishbein, and W. A. Lahoz, Stratospheric transport from the tropics to middle latitudes by planetary-wave mixing, *Nature*, *365*, 533–535, 1993.

Rind, D., and N. K. Balachandran, Modeling the effects of UV variability and the QBO on troposphere-stratosphere system, Part II, The troposphere, *J. Clim*., *8*, 2080–2095, 1995.

Rind, D., R. Suozzo, N. K. Balachandran, A. Lacis, and G. Russell,

The GISS global climate/middle atmosphere model, Part I, Model structure and climatology, *J. Atmos. Sci*., *45*, 329–370, 1988a.

Rind, D., R. Suozzo, and N. K. Balachandran, The GISS global climate/middle atmosphere model, Part II, Model variability due to interactions between planetary waves, the mean circulation and gravity wave drag, *J. Atmos. Sci*., *45*, 371–386, 1988b.

Rosenloff, K. H., and J. R. Holton, Estimates of the stratospheric residual circulation using the downward control principle, *J. Geophys. Res*, *98*, 10,465–10,479, 1993.

Salby, M., and P. Callaghan, Connection between the solar cycle and the QBO: The missing link, *J. Clim*., *12*, in press, 1999.

Salby, M. L., and D. J. Shea, Correlations between solar activity and the atmosphere: An unphysical explanation, *J. Geophys. Res*., *96*, 22,579–22,595, 1991.

Scol, D.-I., and K. Yamazaki, QBO and Pinatubo signals in the mass flux at 100 hPa and stratospheric circulation, *Geophys. Res. Lett*., *25*, 1641–1644, 1998.

Shindell, D., D. Rind, N. Balachandran, J. Lean, and P. Lonergan, Solar variability, Ozone and climate, *Science*, *284*, 305–308, 1999.

Trepte, C. R., and M. H. Hitchman, Tropical stratospheric circulation deduced from aerosol data, *Nature*, *355*, 626–628, 1992.

van Loon, H., and K. Labitzke, Association between the 11-year solar cycle, the QBO, and the atmosphere, Part II, Surface and 700 mbar in the Northern Hemisphere winter, *J. Clim*., *1*, 905–920, 1988.

van Loon, H., and K. Labitzke, The 10–12 year atmospheric oscillation, *Meteorol. Z*., *3*, 259–266, 1994.

van Loon, H., and K. Labitzke, The global range of the stratospheric decadel wave, Part I, Its association with the sunspot cycle in summer and in the annual mean, and with the troposphere, *J. Clim*., *11*, 1529–1537, 1998.

van Loon, H., and K. Labitzke, The signal of the 11-year solar cycle in the global stratosphere, *J. Atmos. Sol. Terr. Phys*., *61*, 53–61, 1999.

N. K. Balachandran, D. Rind, P. Lonergan, and D. T. Shindell, NASA/GISS, 2880 Broadway, New York, NY 10025. (cdnkb@giss.nasa.gov)

(Received January 22, 1999; revised August 9, 1999;
accepted August 17, 1999.)